

# Self-Assembled Containers Based on Extended Tetrathiafulvalene

Sébastien Bivaud, Sébastien Goeb,\* Vincent Croué, Paul I. Dron, Magali Allain, and Marc Sallé\*

LUNAM Université, Université d'Angers, CNRS UMR 6200, Laboratoire MOLTECH-Anjou, 2 bd Lavoisier, 49045 Angers Cedex, France

**S** Supporting Information

**ABSTRACT:** Two original self-assembled containers constituted each by six electroactive subunits are described. They are synthesized from a concave tetratopic  $\pi$ -extended tetrathiafulvalene ligand bearing four pyridyl units and *cis*-M(dppf)(OTf)<sub>2</sub> (M = Pd or Pt; dppf = 1,1'-bis-(diphenylphosphino)ferrocene; OTf = trifluoromethanesulfonate) complexes. Both fully characterized assemblies present an oblate spheroidal cavity that can incorporate one perylene molecule.

Encapsulation of organic guests by discrete molecular cages is subject to an intense interest motivated by applications in various fields, such as chemical sensing, chemical reactivity in confined space, or even guest transport.<sup>1</sup> Nevertheless, the synthetic access to the corresponding 3D receptors is often challenging. From this point of view, the metal-driven self-assembly methodology constitutes a fruitful alternative which has led to a wide diversity of metalla-cages over the past decade.<sup>2</sup>

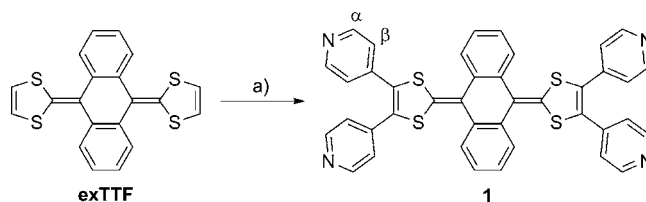
The  $\pi$ -extended tetrathiafulvalene framework (exTTF) exhibits unique geometric and electronic properties.<sup>3</sup> These peculiar features were recently successfully explored by N. Martín et al. who synthesized various macrocyclic covalent receptors incorporating two exTTF units. The resulting curved cavity display a remarkable affinity for fullerenes encapsulation.<sup>3a,4</sup> On this ground and in the course of our studies related to the preparation of electron-rich polygons<sup>5</sup> and polyhedra,<sup>6</sup> we were interested in synthesizing metalla-cages based on the fascinating exTTF building block.

We report herein an expedient synthesis (two steps from the easily available native exTTF) of the first metalla-cages incorporating exTTF units, and we demonstrate the ability of the resulting hosts to encapsulate a polyaromatic perylene guest.

The tetrapyrindyl-exTTF ligand **1** (Scheme 1) was synthesized in one step and in high yield directly from pristine exTTF, through a palladium catalyzed C–H arylation with 4-iodopyridine.<sup>7</sup> Single crystals of the tetratopic ligand could be grown by slow diffusion of hexane in a dichloromethane solution of **1** and an X-ray diffraction study (XRD) was carried out (Figure 2a and SI). Ligand **1** displays the usual exTTF derivative butterfly shape<sup>3</sup> in the crystal, illustrated by a 86° dihedral angle between both 1,3-dithiol-2-ylidene mean plans.

The self-assembly process of tetratopic ligand **1** with *cis*-M(dppf)(OTf)<sub>2</sub> (M = Pd or Pt) complexes was carried out in nitromethane at 40 °C and was monitored by NMR. In both cases, the reaction converged in <1 h into a symmetrical

Scheme 1. Synthesis of Ligand **1**<sup>a</sup>



<sup>a</sup>(a) 4-iodopyridine (5 equiv), cesium carbonate (12 equiv), tri-*tert*-butylphosphonium tetrafluoroborate (0.75 equiv) and palladium(II) acetate (0.25 equiv), dioxane, reflux, 24h, 70%.

discrete species (**2a** (M = Pd) and **2b** (M = Pt)) that could be isolated in high yields (95% and 72%, respectively) by precipitation from diethyl ether. Compared to ligand **1**, compounds **2a** and **2b** present two high-field shifted  $\alpha$  and  $\beta$  pyridine signals<sup>8</sup> in the <sup>1</sup>H NMR spectrum (Figures 1a,b, S4, S9). One singlet is observed for each of the <sup>19</sup>F and <sup>31</sup>P NMR spectra of **2a** and **2b** (Figures S5, S6, S10, S11), and the corresponding DOSY NMR spectra exhibit a single alignment of signals (Figures S8, S12). All these data confirm the formation of only one discrete self-assembled structure in each case. Noteworthy, the diffusion coefficients of **2a** and **2b** are identical and were extracted from the DOSY experiments ( $D \approx 3.3 \times 10^{-10} \text{ m}^2 \cdot \text{s}^{-1}$ ). This observation suggests that both self-assembled structures are of similar size, with an estimated hydrodynamic radius of 10.8 Å from the Stokes–Einstein equation ( $T = 298\text{K}$ ),<sup>9</sup> a value which is compatible with the formation of discrete assemblies of the M<sub>4</sub>L<sub>2</sub> type as shown in Scheme 2.

ESI-FTICR mass spectrometry experiments were carried out with **2a** and **2b** and confirm a M<sub>4</sub>L<sub>2</sub> stoichiometry in the gas phase, as illustrated by the good accordance between isotopic experimental and theoretical patterns (SI) as well as by the characteristic multicharged peaks corresponding to [M-3OTf]<sup>3+</sup> ( $m/z = 1588.6$  (**2a**), 1706.7 (**2b**)) [M-4OTf]<sup>4+</sup> ( $m/z = 1154.3$  (**2a**), 1248.8 (**2b**)), and [M-5OTf]<sup>5+</sup> ( $m/z = 964.4$  (**2b**)) species (Figures S17 and S19). Single crystals of **2a** and **2b** could be grown by slow diffusion of diethyl ether in methanol and acetonitrile respectively. XRD experiments confirm the formation of M<sub>4</sub>L<sub>2</sub> assemblies (Figures 2b,c (**2a**) and S20 (**2b**) and SI) and show in both cases an internal ovoid cavity of ~15 Å long over 9.5 Å width.<sup>10</sup> The ligand unit preserves its butterfly shape within the self-assembled structures but exhibits significantly enhanced curvature compared to **1**, with a dihedral

Received: April 27, 2013

Published: June 24, 2013

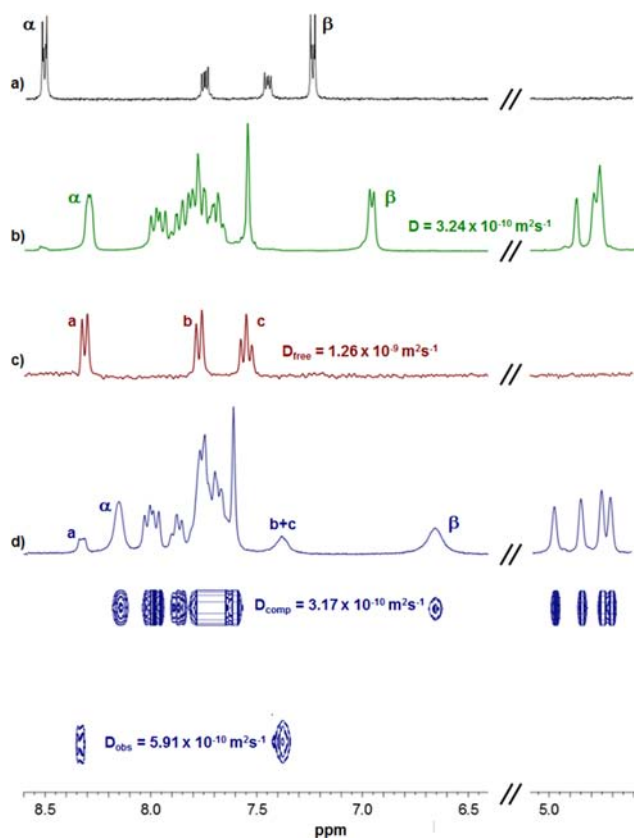
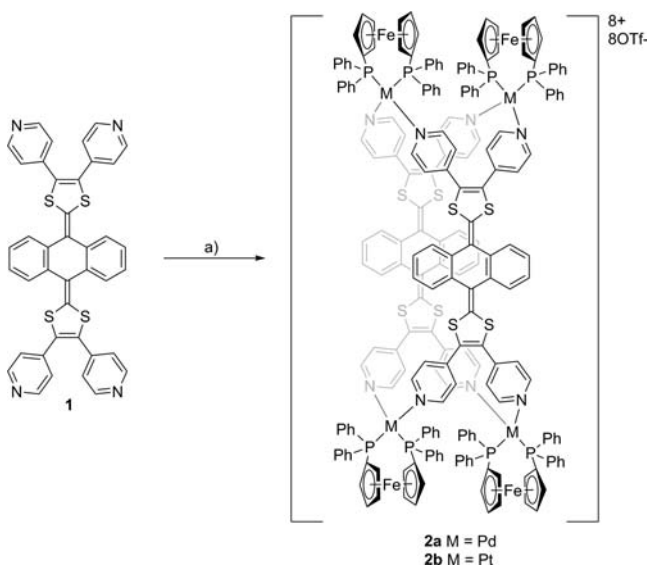


**Figure 1.**  $^1\text{H}$  NMR, downfield region ( $\text{CD}_3\text{NO}_2$ ): (a) **1**, (b) **2a**, (c) perylene (for assignment of a–c signals, see SI), (d) DOSY NMR of a mixture of **2a** and perylene (1/1,  $C = 2 \times 10^{-3}$  M).

### Scheme 2. Synthesis of Cages **2a** and **2b**<sup>a</sup>



<sup>a</sup>(a) *cis*-M(dppf)(OTf)<sub>2</sub> (2 equiv), nitromethane, 40°C; for **2a**, M = Pd, 5 min, 95%; for **2b**, M = Pt, 1 h, 72%.

angle of 56° between the two 1,3-dithiol-2-ylidene mean planes (vs 86° in ligand **1**). This value results in the formation of an elongated cavity suitable for inclusion of planar guests.

Redox properties of ligand **1** as well as of containers **2a** and **2b** were studied by cyclic voltammetry (Figure 3). Ligand **1** shows the usual electrochemical behavior of exTTF derivatives,

i.e., one two e<sup>−</sup> oxidation step to the dicationic species **1**<sup>2+</sup> ( $E_1^{\text{ox}} = 0.30$  V) and a poor electrochemical reversibility on the negative scan, which is due to a geometrical reorganization from a planar fully aromatic species to a folded neutral derivative upon reduction from **1**<sup>2+</sup> to **1**.<sup>3</sup>

Both self-assemblies **2a** and **2b** exhibit two successive oxidation waves attributed to the exTTF core ( $E_1^{\text{ox}} = 0.57$  V (**2a**), 0.65 V (**2b**)) and to the ferrocene units ( $E_2^{\text{ox}} = 0.80$  V), respectively, with four electrons exchanged in each case. Compared to ligand **1**, oxidation of exTTF appears shifted to higher potential (+0.26 V (**2a**) and +0.34 V (**2b**)) and is not reversible. These two features are attributed to conjunction of two factors: (i) coordination to metal centers contributes to reduce the  $\pi$ -donating character of redox exTTF units ( $E_1^{\text{ox}}$  increasing), and (ii) the rigid character of the self-assembled structures **2a,b** presumably hampers the redox-driven conformational changes of the exTTF components which is usually observed with isolated exTTF derivatives. Interestingly, no change of the voltammograms was observed upon sequential redox cycling, outlining the chemical robustness of the self-assembled systems **2a,b**.

A remarkable feature of exTTF-based covalent macrocycles<sup>3a,4</sup> is their ability to bind guests in the cavity defined by the anthracenyl surface of their exTTF components. It is worth noting that in the case of containers **2a** and **2b**, the cavity surface is defined by the other concave fragment of the exTTF framework, i.e., the one containing both 1,3-dithiol rings. Regarding the shape and the size of the ovoid cavity of **2a** and **2b**, inclusion of planar polyaromatic guests, such as pyrene, coronene, and perylene, was studied by NMR spectroscopy (Figures 1d and S14–S16). Whereas no effect was observed with pyrene and coronene, the  $^1\text{H}$  NMR spectrum of a stoichiometric  $\text{CD}_3\text{NO}_2$  mixture of containers **2a** (or **2b**) and perylene appears notably modified compared to those of the individual components (Figures 1b–d and S14, S16). The H $\alpha$  and H $\beta$  pyridine signals are upshifted in the case of complexing cages **2a** and **2b** and become larger, as expected for a rapid exchange at the NMR time scale, which is confirmed by a COSY experiment (Figure S15). Likewise, the b and c perylene protons are fused into a single signal at 7.35 ppm upon encapsulation. Considering the cavity size, a 1:1 binding process was expected, which was confirmed by a ESI-FTICR mass spectrometry study upon analyzing a stoichiometric mixture of both entities (Figures 4 and S18).<sup>11</sup> Peaks at  $m/z = 1014$ , 1305 (**2b**), and 1218 (**2a**) confirm inclusion of one perylene unit into the ovoid cavity. The association constants of the host–guest 1:1 inclusion complexes peryleneC**2a** and peryleneC**2b** could be determined from DOSY NMR titration experiments in  $\text{CD}_3\text{NO}_2$ , from a 1/1 ratio of host–guest mixtures (Figures 1d and S13, S15).<sup>12</sup> From these data (Table S1),  $K_a$  values of  $3.9 \pm 0.1 \times 10^3$  (**2a**) and  $3.2 \pm 0.1 \times 10^3$  (**2b**) could be calculated.

In summary, an expedient two-step procedure is described to reach the first examples of self-assembled 3D structures based on the electron-rich exTTF system. The first step involves a direct tetra-functionalization of pristine exTTF to afford the tetratopic ligand **1**. The latter is then engaged in a metal-driven self-assembly procedure to reach stable containers **2a** and **2b**, which were characterized in solution as well as in the solid state. Containers **2a** and **2b**, whose internal cavity is ovoid and is surrounded by six redox-active electron-donating units, are stable upon successive oxidation–reduction cycling and show a good ability to include one perylene molecule. Considering the

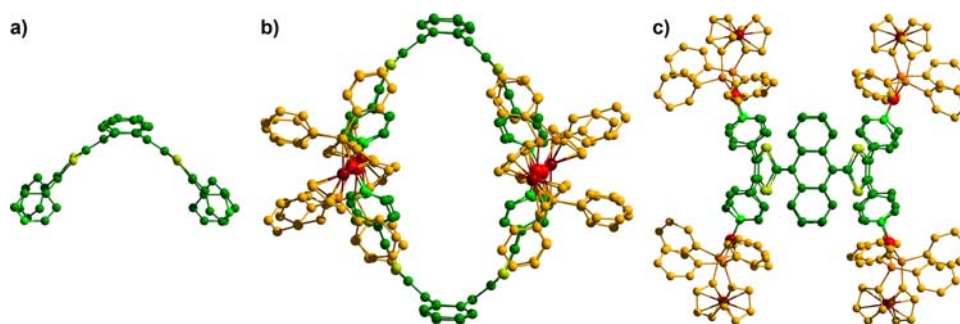


Figure 2. X-ray crystal structures of: (a) ligand **1**, (b) host structure **2a** (lateral view), and (c) **2a** (top view).

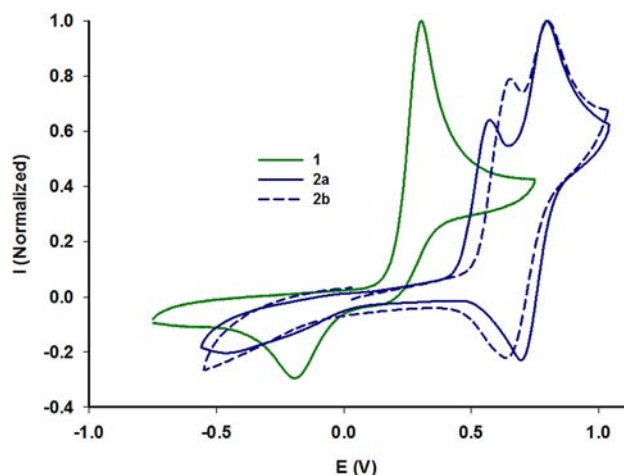


Figure 3. Cyclic voltammogram of ligand **1** ( $C = 10^{-3}$  M,  $\text{CH}_3\text{CN}/\text{CH}_2\text{Cl}_2$ , 0.1 M  $n\text{Bu}_4\text{NPF}_6$ ,  $100 \text{ mV}\cdot\text{s}^{-1}$ , Pt) and of containers **2a** and **2b** ( $C = 10^{-3}$  M,  $\text{CH}_3\text{CN}$ , 0.1 M  $n\text{Bu}_4\text{PF}_6$ ,  $100 \text{ mV}\cdot\text{s}^{-1}$ , Cgr), V vs Fc/Fc<sup>+</sup>.

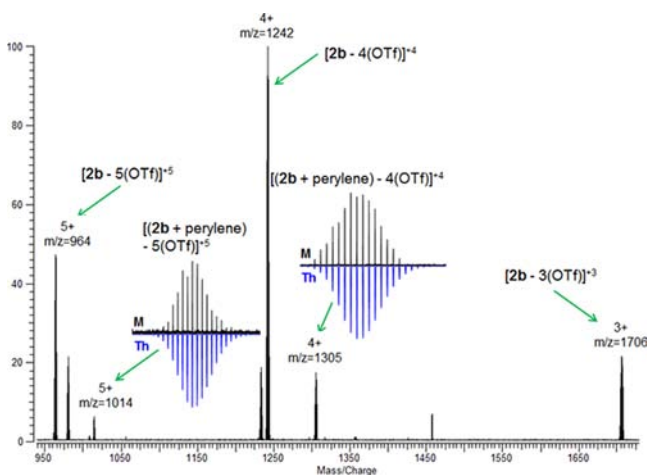


Figure 4. ESI-FTICR of the stoichiometric mixture of **2b** with perylene in  $\text{CH}_3\text{CN}$  ( $C = 10^{-3}$  M).

recent success of 2D exTTF covalent receptors in host–guest chemistry<sup>4</sup> and regarding the easy synthetic access to ligand **1** as well as to cages **2a** and **2b** through the metal-assisted strategy, we believe that such results are topical and open promising opportunities toward new 3D receptors designed on purpose for the binding of given neutral molecules.

## ■ ASSOCIATED CONTENT

### ● Supporting Information

Detailed synthesis protocols, experimental methods, and characterization data. This material is available free of charge via the Internet at <http://pubs.acs.org>.

## ■ AUTHOR INFORMATION

### Corresponding Author

[marc.salle@univ-angers.fr](mailto:marc.salle@univ-angers.fr); [sebastien.goeb@univ-angers.fr](mailto:sebastien.goeb@univ-angers.fr)

### Notes

The authors declare no competing financial interest.

## ■ ACKNOWLEDGMENTS

The authors gratefully acknowledge the CNRS and the Région des Pays de la Loire for a PhD grant (S.B.) as well as the PIAM (Univ. Angers) and the TGE FT-ICR (Drs. Frédéric Aubriet and Vincent Carré, CNRS-Univ. Lorraine) for their assistance in spectroscopic analyses, and finally the Johnson-Matthey company for their generous providing of palladium and platinum salts.

## ■ REFERENCES

- (1) (a) Molecular Encapsulation: *Organic Reactions in Constrained Systems*, John Wiley & Sons, Ltd: Hoboken, NJ, 2010. (b) Steed, J. W.; Atwood, J. L. *Supramolecular Chemistry*; John Wiley and Sons: Hoboken, NJ, 2009; p 307.
- (2) Recent reviews: (a) Amouri, H.; Desmarets, C.; Moussa, J. *Chem. Rev.* **2012**, *112*, 2015. (b) MacGillivray, L. R. *Angew. Chem., Int. Ed.* **2012**, *51*, 1110. (c) Chakrabarty, R.; Mukherjee, P. S.; Stang, P. J. *Chem. Rev.* **2011**, *111*, 6810. (d) Inokuma, Y.; Kawano, M.; Fujita, M. *Nat. Chem.* **2011**, *3*, 349. (e) Jin, P.; Dalgarno, S. J.; Atwood, J. L. *Coord. Chem. Rev.* **2010**, *254*, 1760. (f) De, S.; Mahata, K.; Schmittl, M. *Chem. Soc. Rev.* **2010**, *39*, 1555. (g) Therrien, B. *Eur. J. Inorg. Chem.* **2009**, *2009*, 2445. (h) Northrop, B. H.; Zheng, Y.-R.; Chi, K.-W.; Stang, P. J. *Acc. Chem. Res.* **2009**, *42*, 1554. (i) Stang, P. J. *J. Org. Chem.* **2009**, *74*, 2. (j) Yoshizawa, M.; Klosterman, J. K.; Fujita, M. *Angew. Chem., Int. Ed.* **2009**, *48*, 3418. (k) Han, Y.-F.; Jia, W.-G.; Yu, W.-B.; Jin, G.-X. *Chem. Soc. Rev.* **2009**, *38*, 3419. (l) Northrop, B. H.; Chercka, D.; Stang, P. J. *Tetrahedron* **2008**, *64*, 11495. (m) Northrop, B. H.; Yang, H.-B.; Stang, P. J. *Chem. Commun.* **2008**, *0*, 5896. (n) Cooke, M. W.; Chartrand, D.; Hanan, G. S. *Coord. Chem. Rev.* **2008**, *252*, 903. (o) Dalgarno, S. J.; Power, N. P.; Atwood, J. L. *Coord. Chem. Rev.* **2008**, *252*, 825. (p) Zangrando, E.; Casanova, M.; Alessio, E. *Chem. Rev.* **2008**, *108*, 4979.
- (3) (a) Brunetti, F. G.; Lopez, J. L.; Atienza, C.; Martin, N. J. *Mater. Chem.* **2012**, *22*, 4188. (b) Moore, A. J.; Bryce, M. R. *J. Chem. Soc., Perkin Trans. 1* **1991**, *0*, 157. (c) Bryce, M. R.; Moore, A. J.; Hasan, M.; Ashwell, G. J.; Fraser, A. T.; Clegg, W.; Hursthouse, M. B.; Karaulov, A. I. *Angew. Chem., Int. Ed. Engl.* **1990**, *29*, 1450.
- (4) (a) Canevet, D.; Pérez, E. M.; Martín, N. *Angew. Chem., Int. Ed.* **2011**, *50*, 9248. (b) Canevet, D.; Gallego, M.; Isla, H.; de Juan, A.;

Pérez, E. M.; Martín, N. *J. Am. Chem. Soc.* **2011**, *133*, 3184. (c) Isla, H.; Gallego, M.; Pérez, E. M.; Viruela, R.; Ortí, E.; Martín, N. *J. Am. Chem. Soc.* **2010**, *132*, 1772.

(5) (a) Goeb, S.; Bivaud, S.; Dron, P. I.; Balandier, J.-Y.; Chas, M.; Salle, M. *Chem. Commun.* **2012**, *48*, 3106. (b) Balandier, J.-Y.; Chas, M.; Goeb, S.; Dron, P. I.; Rondeau, D.; Belyasmine, A.; Gallego, N.; Salle, M. *New J. Chem.* **2011**, *35*, 165.

(6) Bivaud, S.; Balandier, J.-Y.; Chas, M.; Allain, M.; Goeb, S.; Sallé, M. *J. Am. Chem. Soc.* **2012**, *134*, 11968.

(7) Mitamura, Y.; Yorimitsu, H.; Oshima, K.; Osuka, A. *Chem. Sci.* **2011**, *2*, 2017.

(8) Mishra, A.; Ravikumar, S.; Hong, S. H.; Kim, H.; Vajpayee, V.; Lee, H.; Ahn, B.; Wang, M.; Stang, P. J.; Chi, K.-W. *Organometallics* **2011**, *30*, 6343.

(9) Cohen, Y.; Avram, L.; Frish, L. *Angew. Chem., Int. Ed.* **2005**, *44*, 520.

(10) Distances between both central cycles of the anthraquinone unit and between two facing metal centers, respectively.

(11) Meng, W.; Breiner, B.; Rissanen, K.; Thoburn, J. D.; Clegg, J. K.; Nitschke, J. R. *Angew. Chem., Int. Ed.* **2011**, *50*, 3479.

(12) Fielding, L. *Tetrahedron* **2000**, *56*, 6151.